Theoret. Chim. Acta (Berl.) 44, 351–373 (1977)

THEORETICA CHIMICA ACTA
© by Springer-Verlag 1977

Natural Spin Orbital Analysis of Diatomic Molecular Wave Functions in Terms of Generalized Diatomic Orbitals

II. Energy and Occupation Number Curves for Excited States of H_2*

Siegfried Kehl and Klaus Helfrich

I. N. Stranski Institute for Physical and Theoretical Chemistry, Technical University of Berlin, Ernst-Reuter-Platz 7, D-1000 Berlin 10, Federal Republic of Germany

Hermann Hartmann

Arbeitsstelle für theoretische Chemie bei der Akademie der Wissenschaften und der Literatur zu Mainz, Auf der Platt 53, D-6246 Glashütten (Ts) 1, Federal Republic of Germany

Starting from the demi-H_2^+-model for Rydberg states, *ab initio* calculations of the energy and the wave function for some excited states of H_2 have been carried out with the help of diatomic orbitals. The potential curves and wave functions for the following states: $2^1\Sigma_g^+$, $3^1\Sigma_g^+$, $1^3\Sigma_g^+$, $2^3\Sigma_g^+$, $1^1\Sigma_u^+$, $2^1\Sigma_u^+$, $1^3\Sigma_u^+$, $2^3\Sigma_u^+$, $3^3\Sigma_u^+$, $1^1\Pi_g$, $1^3\Pi_g$, $1^1\Pi_u$ and $1^3\Pi_u$ have been calculated by a complete CI (configuration interaction) calculation in the sense that all configurations of the state symmetry have been used which can be formed from a given basis set. From the wave functions thus obtained the natural spin orbitals are calculated subsequently to the variational calculations. The dependence of the occupation numbers of the natural spin orbitals on internuclear distance is interpreted according to the model and is used for the explanation of the special features like double minima and maxima which occur in the potential curves of H_2. For the curves of the occupation numbers a non-crossing rule in analogy to that for potential curves is valid. The potential curves for the states $1^3\Pi_g$ and $1^3\Pi_u$ have been improved by the use of linear combinations of diatomic orbitals with different nuclear charges, which allow a flexible transition to linear combinations of atomic orbitals.

Key words: Natural orbital analysis – Diatomic orbitals – H_2, excited states of ~

1. Introduction

For the ground state of the H_2 molecule numerous natural orbital (NO) analyses of the wave function are contained in the literature (see survey in [1], p. 253). Although

* Dedicated to Professor Iwan N. Stranski on the occasion of his 80th birthday.

there are also calculations of excited states for the H_2 molecule, only a few natural orbital analyses for limited ranges of internuclear distance can be found for these states [1-3]. An analysis of this kind for an extended region of internuclear distance has been carried out for the state $1^3\Sigma_u^+$ [4]. For those excited states which have been analysed in [3] at the nuclear distance $R = 2.0$[1] a similarity of the NO's with functions from a H_2^+-type model has been found. The calculations of some low-lying excited states of H_2 are extended here to a greater range of the internuclear distance R. The suitability of H_2^+-type and other diatomic orbitals as basis functions for variational calculations as well as for NO analyses of these two-electron states is examined.

2. Theory

The Rydberg states of the H_2 molecule have been discussed by Mulliken [5] with the help of the demi-H_2^+-model. This idea is based on the work of Hylleraas [6] in which approximate functions of the following form have been used for the calculation of the ground state and some excited states of H_2:

$$\Psi = 1/\sqrt{2}(|\chi_1\overline{\chi_2}| \pm |\overline{\chi_1}\chi_2|) \tag{1}$$

χ_1 and χ_2 are the exact solutions for the ground state and the excited state respectively for the one-electron two-centre problem with the nuclear charge $Z(\chi_1) = 1$ and $Z(\chi_2) = 0.5$. For calculations of potential curves for excited states of H_2, more general basis functions are used here. These generalized diatomic orbitals (GDO's) are defined as the exact solutions of the one-particle Schrödinger equation

$$\left\{-\frac{\Delta}{2} - \frac{Z_a}{r_a} - \frac{Z_b}{r_b} - \frac{Q}{r_a r_b}\right\}\chi = \epsilon\chi \tag{2}$$

belonging to negative energy eigenvalues ϵ. The additional potential $Q/(r_a r_b)$ is a special case of the core potential which has been proposed by Lassettre and Peek [7] and by Teller and Sahlin [8] as a model potential in one-electron theories for many-electron molecules. The eigenfunctions of Eq. (2) are specified as

$$\chi = |nl\gamma_s; Z_a, Z_b, Q) \tag{3}$$

where n and l are the quantum numbers of the united atom; γ is an irreducible representation of $C_{\infty v}$ (or $D_{\infty h}$ if $Z_a = Z_b$) and s is the sign of the eigenvalue of the z-component of the angular momentum. The solutions of Eq. (2) are derived by semi-analytical methods described previously [9-11]. The basis functions given by Eq. (3) contain three non-linear parameters Z_a, Z_b and Q. However, some preliminary calculations [12] showed that the consideration of Q as a variational parameter did not improve the results in general as is the case for the ground state of the molecules H_2, HeH^+ and He_2 [13, 14]. Therefore at most two non-linear parameters have been opti-

[1] All distances and energies in atomic units.

mized. Most generally symmetry-adapted linear combinations of two DO's [14] are used as basis functions in the present work:

$$|nl\gamma(D_{\infty h}); Z_a, Z_b, 0\rangle = N_{\pm}\{|nl\gamma(C_{\infty v}); Z_a, Z_b, 0) \pm |nl\gamma(C_{\infty v}); Z_b, Z_a, 0)\} \qquad (4)$$

where $N_{\pm}$ is a normalization factor.

Basis functions of the type given in Eq. (3) with $Q = 0$ and in Eq. (4) are used within the framework of configuration interaction (CI) calculations (after Gram-Schmidt orthogonalization). All the DO's are used in these calculations which are necessary to guarantee a correct asymptotic behaviour of the potential curves for $R \to 0$ and $R \to \infty$. In addition those configurations are taken into account which may have similar energies to that of the state under consideration for medium internuclear distances. Therefore it is advantageous to minimize two or more energy values together. In each of the calculations all configurations are used which can be formed from a given basis set ("complete" CI). The basis functions chosen in this way are given under the headings of the states which are calculated.

From the many-electron wave functions thus obtained the natural spin orbitals (NSO's) are calculated subsequently (see [12, 13]). The natural orbitals, which differ in the two-electron case from the natural spin orbitals only by a simple α- or β-spin factor, can be classified in accordance with the theorems of Bingel and Kutzelnigg [15]. They are interpreted in terms of the occupation numbers for a greater region of the internuclear distance according to the model above and are used for an explanation of the special features of the potential curves for excited states of H_2 like double minima and maxima.

The curves of the occupation numbers as functions of the internuclear distance show the following behaviour: if the spatial part of the wave function for the two-electron system belongs to a one-dimensional irreducible representation of the symmetry group of the linear molecule (e.g. Σ, Π^+; for H_2 such a choice is always possible), then the one-particle density matrix is factorized according to symmetry types [16]. Because of the Hermiticity of the one-particle density matrix the derivation of the non-crossing rule of Wigner and von Neumann [17] remains valid here for its eigenvalues, the occupation numbers. The curves of the occupation numbers as functions of the internuclear distance belonging to NSO's (or NSO space parts, here NO's) of the same spatial symmetry (e.g. $|1\sigma_g)$ and $|2\sigma_g)$) will not cross *in general* whereas crossings of occupation number curves belonging to NO's of different symmetry (e.g. $|1\sigma_g)$ and $|1\sigma_u)$) may occur. As far as two-electron systems are concerned additional degeneracies of the occupation numbers (for all internuclear distances) may occur as has been shown by Bingel and Kutzelnigg [16, 18]. Then for all internuclear distances NO's of different symmetry type belong to the same occupation number (e.g. for $2^1\Sigma_u^+$ $|1\sigma_g)$ and $|1\sigma_u)$ as well as $|2\sigma_g)$ and $|2\sigma_u)$). The different blocks of the density matrix are not affected by this so that the occupation number curves belonging to $|1\sigma_g)$ and $|2\sigma_g)$ and those belonging to $|1\sigma_u)$ and $|2\sigma_u)$ will not cross; similarly for the curves belonging to ($|1\sigma_g)$, $|1\sigma_u)$) and to ($|2\sigma_g)$, $|2\sigma_u)$). Moreover the $^3\Sigma_g^+$-states show an additional degeneracy so that two NO's of equal symmetry belong to one occupation number [18]. Therefore the general case is not given. However, further degeneracies are not to be expected.

Examples for the non-crossing rule of occupation numbers can be found for the states $2^1\Sigma_g^+$, $3^1\Sigma_g^+$, $2^1\Sigma_u^+$, $2^3\Sigma_u^+$ and $3^3\Sigma_u^+$ (see below).

3. Results

Energy and occupation number curves have been calculated for the following low-lying Σ- and Π-states of H_2: $2^1\Sigma_g^+$, $3^1\Sigma_g^+$, $1^3\Sigma_g^+$, $2^3\Sigma_g^+$, $1^1\Sigma_u^+$, $2^1\Sigma_u^+$, $1^3\Sigma_u^+$, $2^3\Sigma_u^+$, $3^3\Sigma_u^+$, $1^1\Pi_g$, $1^1\Pi_u$, $1^3\Pi_g$ and $1^3\Pi_u$. The calculations have been performed for the range of the internuclear distance from 0.5 (or 1.0) to 14.0 in steps of 1.0, 0.5 or 0.25 according to the special features of the energy or occupation number curves in a certain region. For each value of R one common non-linear parameter Z_{opt} of the excited orbitals of the H_2^+-type diatomic orbital basis set (HTDO; $Z_a = Z_b = Z_{\text{opt}}$ in Eqs. (2) and (3)) has been optimized. The nuclear charge of the $|1s\sigma_g)$-orbital (and of a second $|2p\sigma_u)$-orbital in some of the calculations) has been kept constant. In addition linear combinations of DO's (LCDO's) have been used for the Π-states. The HTDO's contain five non-zero coefficients in the expansion of their μ- and ν-part (μ, ν: prolate spheroidal coordinates) [9–11]. Some pilot calculations have shown that the energy values do not change within five places if the number of these expansion coefficients is increased.

Tables containing the calculated optimal variational parameters Z_{opt}, the energies, occupation numbers and coefficients of the expansion of the natural orbitals in terms of the HTDO's are to be found in [12] and are available on request. Figures of the potential and occupation number curves are given here only for a visualization of the results.

3.1. $2^1\Sigma_g^+$, $3^1\Sigma_g^+$

The basis set of HTDO's for the simultaneous calculation of the states $2^1\Sigma_g^+$ E, F and $3^1\Sigma_g^+$ was set up to take into account the mixing of the functions $1s\sigma_g 2s\sigma_g\,{}^1\Sigma_g^+$ and $1s\sigma_g 3s\sigma_g\,{}^1\Sigma_g^+$ as well as $1s\sigma_g 3d\sigma_g\,{}^1\Sigma_g^+$. For the second minimum $2^1\Sigma_g^+$ F the configuration $(2p\sigma_u)^2$ is of great importance. In addition at greater internuclear distances the doubly excited configurations $(2p\sigma_u 3p\sigma_u)$ and $(2p\sigma_u 4f\sigma_u)$ have to be taken into account because the HTDO's $|3p\sigma_u)$ and $|4f\sigma_u)$ are degenerate for $R \to \infty$ with $|2s\sigma_g)$, $|3s\sigma_g)$, $|3d\sigma_g)$ respectively. A second $|2p\sigma_u')$ is used (in addition to $|2p\sigma_u)$) in analogy to the double-zeta method with the fixed value of $Z = 1.0$. The nuclear charge for the core function $|1s\sigma_g)$ is also kept constant at $Z = 1.0$.

Summing up, the following basis set has been used:

$$|1s\sigma_g; 1.0, 1.0, 0), \quad |2s\sigma_g; Z_{\text{opt}}, Z_{\text{opt}}, 0), \quad |3s\sigma_g; Z_{\text{opt}}, Z_{\text{opt}}, 0), \quad |3d\sigma_g; Z_{\text{opt}}, Z_{\text{opt}}, 0),$$
$$|2p\sigma_u; Z_{\text{opt}}, Z_{\text{opt}}, 0), \quad |3p\sigma_u; Z_{\text{opt}}, Z_{\text{opt}}, 0), \quad |4f\sigma_u; Z_{\text{opt}}, Z_{\text{opt}}, 0), \quad |2p\sigma_u'; 1.0, 1.0, 0).$$

The potential curves and the curves of the occupation numbers are given in Fig. 1 and Fig. 2a, b respectively. In most cases the energy values from the literature [2, 19–21] are better than the present results for $2^1\Sigma_g^+$. For $3^1\Sigma_g^+$ they are improved here in comparison with the results of Davidson [2].

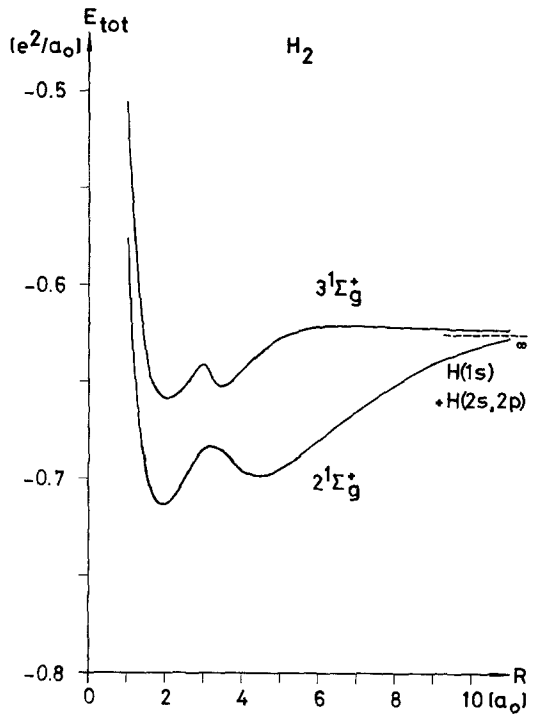

Fig. 1. Potential curves of the states $2^1\Sigma_g^+$ and $3^1\Sigma_g^+$ of H_2

Fig. 2b

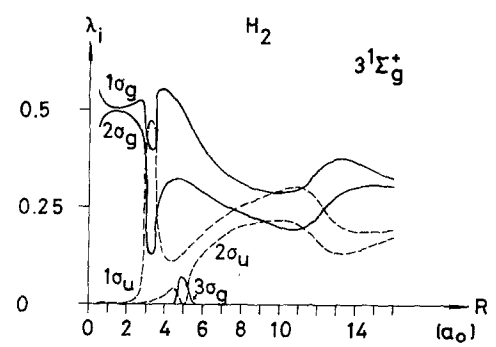

Fig. 2a

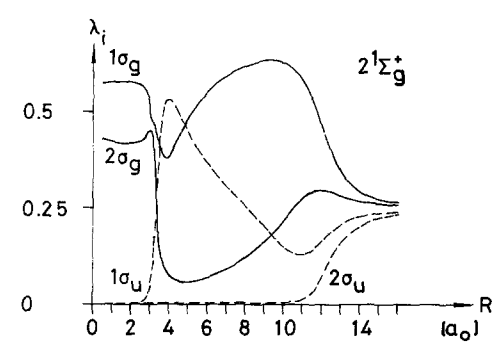

Fig. 2a and b. Occupation numbers λ_i as functions of the internuclear distance R. a) Results for the state $2^1\Sigma_g^+$; b) results for the state $3^1\Sigma_g^+$

If the basis is enlarged by the functions $|2p\pi_u)$ and $|3d\pi_g)$ and the non-linear parameters are optimized extensively [12] a value of $E_{tot} = -0.65583$ for the total energy of $3^1\Sigma_g^+$ is obtained at $R = 3.5$. Below this energy value there is only one experimental state with an equilibrium distance of this size namely $(2p\pi_u)^2\,?^1\Sigma_g^+\,3^1K$ with $E_{tot} = -0.66117$ [22a, b]. On the basis of the NO-analysis such a simple assignment like $(2p\pi_u)^2$ does not seem adequate because there are no strongly occupied π_u-type orbitals.

3.2. $1^3\Sigma_g^+$, $2^3\Sigma_g^+$

For the calculation of the two states $1^3\Sigma_g^+$ and $2^3\Sigma_g^+$ the same basis set as listed above for the corresponding singlet states has been used. The parameter Z_{opt} has been optimized independently here.

The great maximum (at $R \approx 5.25$) [23, 24] in the potential curve for the state $2^3\Sigma_g^+$ and the dissociative behaviour of the two states is reproduced correctly (see Fig. 3). The flat maximum at $R \approx 8.0$ of the curve of the state $1^3\Sigma_g^+$ is due to the model basis set because it has been found neither experimentally nor theoretically [25]. If the basis is changed in the same way as has been done for some of the Π-states a disappearance of the maximum can be expected. The corresponding occupation number curves are given in Fig. 4a, b.

3.3. $1^1\Sigma_u^+$, $2^1\Sigma_u^+$

A complete CI calculation has been carried out with a basis set that allows the right behaviour of the potential curve for $R \to 0$ and $R \to \infty$. This basis set consists of the functions:

$$|1s\sigma_g; 1.0, 1.0, 0), \quad |2s\sigma_g; Z_{opt}, Z_{opt}, 0), \quad |3d\sigma_g; Z_{opt}, Z_{opt}, 0),$$
$$|2p\sigma_u; Z_{opt}, Z_{opt}, 0), \quad |3p\sigma_u; Z_{opt}, Z_{opt}, 0), \quad |4f\sigma_u; Z_{opt}, Z_{opt}, 0);$$

the HTDO $|4p\sigma_u; Z_{opt}, Z_{opt}, 0)$ is added to this set in order to take into account the mixing with the main configuration of $1s\sigma_g 4p\sigma_u 3^1\Sigma_u^+ B''$. In order to make possible a comparison the states $1^3\Sigma_u^+$, $2^3\Sigma_u^+$ and $3^3\Sigma_u^+$ have been calculated with the same basis set (see below).

The resulting potential curves show minima at the internuclear distances $R_e = 2.3$ and $R_e = 2.05$ respectively (see Fig. 5). The maximum which has been obtained here for the state $2^1\Sigma_u^+ B'$ at $R \approx 5.0$ is not found experimentally [26, 27]. However, discrepancies between experimental and theoretical results may arise as the example of the state $1^1\Sigma_u^+ B$ shows [28]. The corresponding occupation number curves are represented in Fig. 6a, b.

3.4. $1^3\Sigma_u^+$, $2^3\Sigma_u^+$, $3^3\Sigma_u^+$

The calculations with the same basis set of HTDO's as for the $^1\Sigma_u^+$-states show the following results: as a special feature a slight maximum occurs in the potential curve of $2^3\Sigma_u^+$ at $R \approx 6.0$ similar to the maxima of $2^1\Sigma_u^+$, $1^3\Sigma_g^+$ and $3^1\Sigma_g^+$ (see Fig. 7). The potential curve of $3^3\Sigma_u^+$ shows a large maximum (like that for $2^3\Sigma_g^+$ and $1^3\Pi_g$ (see

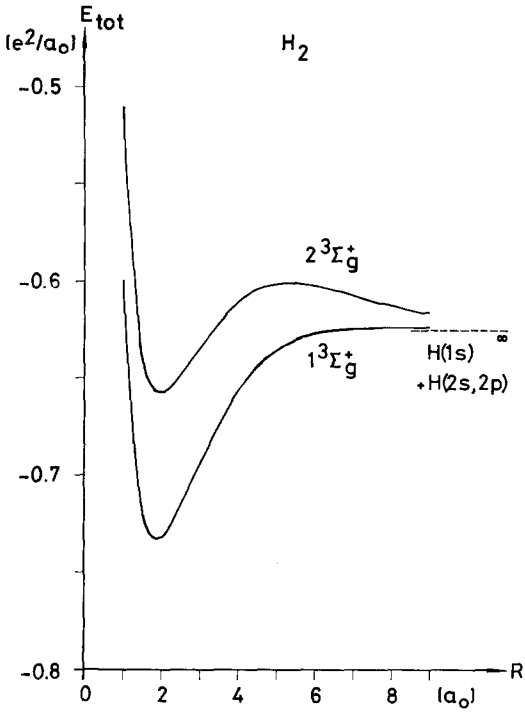

Fig. 3. Potential curves for the states $1^3\Sigma_g^+$ and $2^3\Sigma_g^+$ of H_2

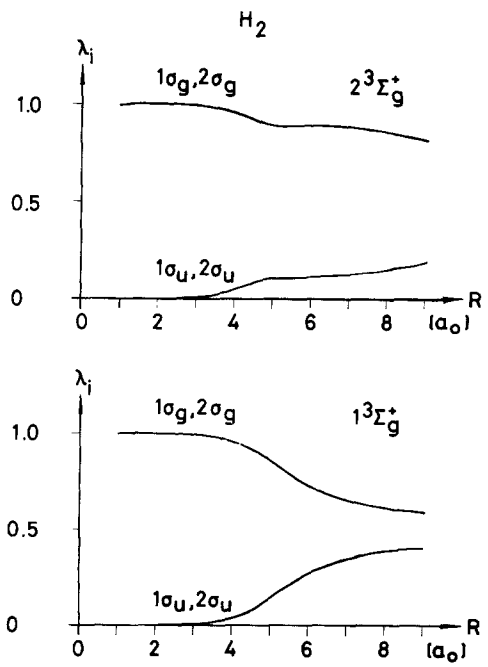

Fig. 4b

Fig. 4a

Fig. 4a and b. Occupation numbers λ_i as functions of the internuclear distance R. a) Results for the state $1^3\Sigma_g^+$; b) results for the state $2^3\Sigma_g^+$

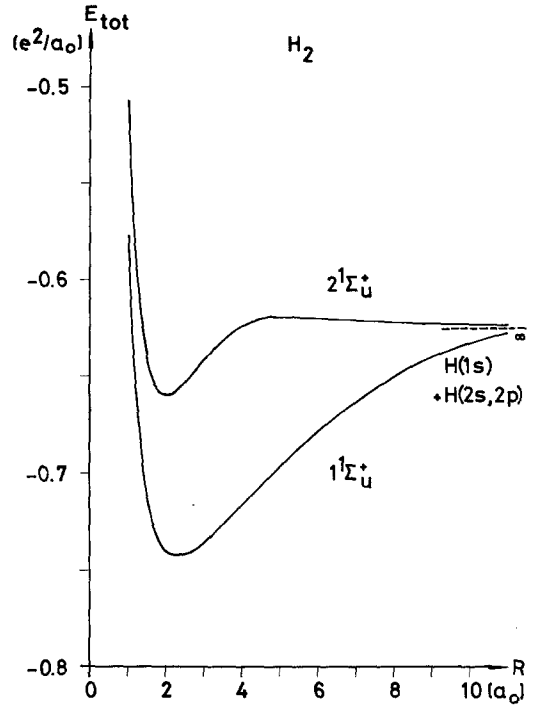

Fig. 5. Potential curves for the states $1^1\Sigma_u^+$ and $2^1\Sigma_u^+$ of H_2

Fig. 6b

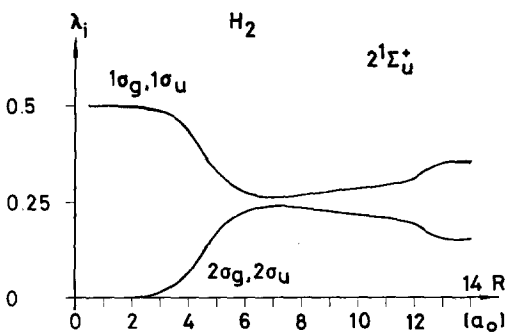

Fig. 6a

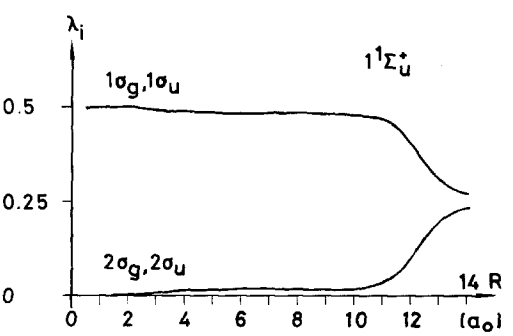

Fig. 6a and b. Occupation numbers λ_i as functions of the internuclear distance R. a) Results for the state $1^1\Sigma_u^+$; b) results for the state $2^1\Sigma_u^+$

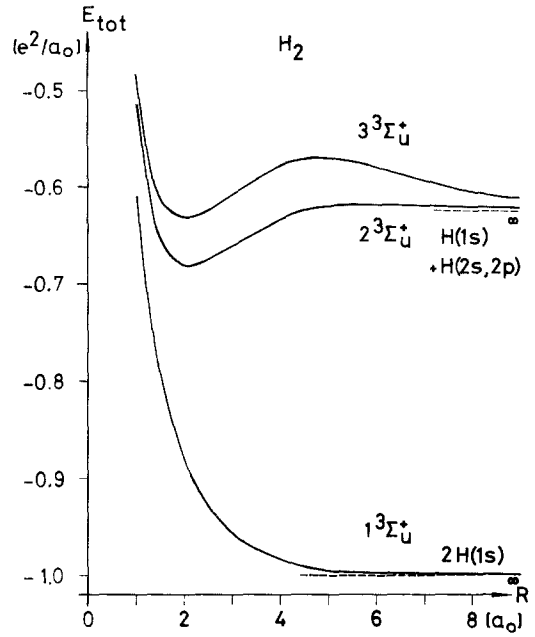

Fig. 7. Potential curves for the states $1^3\Sigma_u^+$, $2^3\Sigma_u^+$ and $3^3\Sigma_u^+$ of H_2

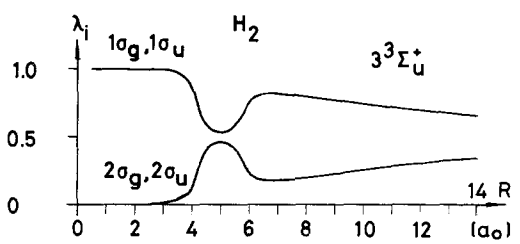

Fig. 8c

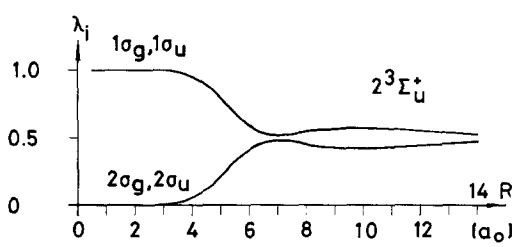

Fig. 8b

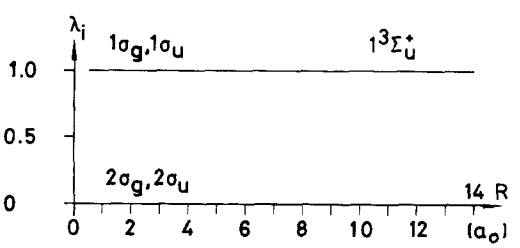

Fig. 8a

Fig. 8a–c. Occupation numbers λ_i as functions of the internuclear distance R. a) Results for the state $1^3\Sigma_u^+$; b) results for the state $2^3\Sigma_u^+$; c) results for the state $3^3\Sigma_u^+$

below)) at $R \approx 4.8$. An experimental potential curve of the state $2^3\Sigma_u^+$ is contained in [22b]. Theoretical calculations exist for $1^3\Sigma_u^+$, $2^3\Sigma_u^+$ and $3^3\Sigma_u^+$ [3, 22b, 23, 28–31]. The occupation number curves for the three states are given in Fig. 8a, b, c.

3.5. $1^3\Pi_u$, $1^3\Pi_g$; $1^1\Pi_u$, $1^1\Pi_g$

It is possible to study the occurrence of maxima and to compare different methods with an especially small basis for the lowest $^3\Pi$-states. The corresponding $^1\Pi$-states have been compared for some of the calculations. The smallest possible HTDO-basis set for complete CI calculations of all these states (the functions $|1s\sigma_g, 1.0, 1.0, 0)$, $|2p\sigma_u; 1.0, 1.0, 0)$, $|2p\pi_u^+, Z_{\text{opt}}, Z_{\text{opt}}, 0)$, $|3d\pi_g^+; Z_{\text{opt}}, Z_{\text{opt}}, 0))$ has been chosen. In the present case the NO's coincide with the basis functions with the given symmetry because of the small basis set.

The two states $1^3\Pi_g$ and $1^1\Pi_g$ each possess a maximum at $R \approx 4.5$ (see Figs. 9, 10) which has also been obtained in previous theoretical papers ([31, 32]; [23]: only $1^3\Pi_g$). The second flat minimum for the state $1^1\Pi_g$ ([5b], [26]) did not result here because of the very small basis set. The slight maximum at $R \approx 7.0$ for $1^1\Pi_u$ has been found experimentally [29, 33] and theoretically [34–37] (see [5b] and the references given there).

If a LCDO basis set is used which allows a flexible transition to LCAO functions the resulting potential curve of the state $1^3\Pi_u$ no longer shows a maximum (see also [22b]). This is confirmed by other variational calculations contained in the literature [34, 36]. Instead of

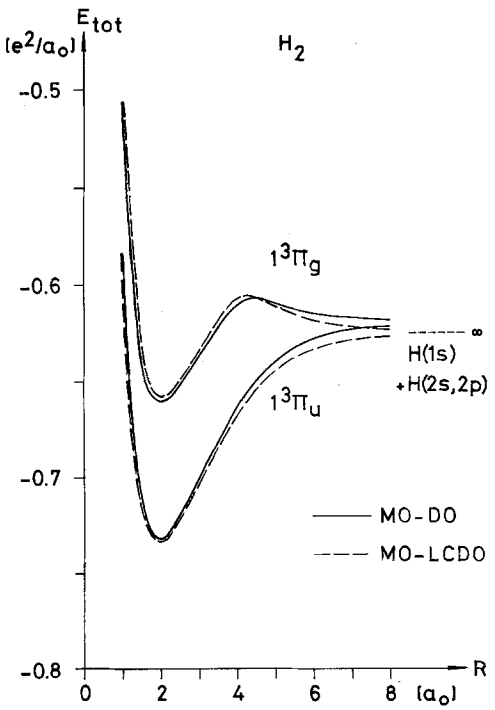

Fig. 9. Potential curves of the states $1^3\Pi_u$ and $1^3\Pi_g$ of H_2. Results of the MO-DO and of the MO-LCDO calculation

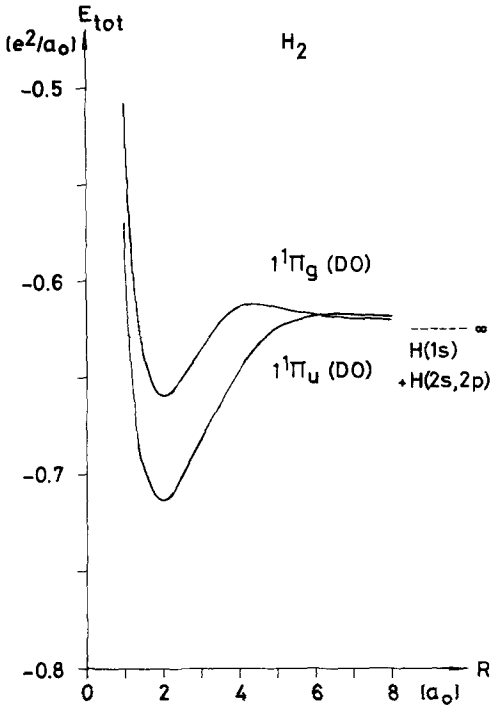

Fig. 10. Potential curves of the states $1^1\Pi_u$ and $1^1\Pi_g$ of H_2 calculated by the MO-DO method

a single HTDO $|2p\pi_u^+; Z_{\text{opt}}, Z_{\text{opt}}, 0)$ and $|3d\pi_g^+; Z_{\text{opt}}, Z_{\text{opt}}, 0)$, a linear combination is used which consists of two DO's with different nuclear charges $|2p\pi^+; Z_a, Z_b, 0)$ and $|2p\pi^+; Z_b, Z_a, 0)$. This procedure is called the MO-LCDO method in contrast to the earlier MO-DO method [14]. The correct linear combinations emerge from the CI calculation. The occupation number curves for all the Π-states calculated by the MO-DO method are given in Figs. 11 and 12; those obtained by the MO-LCDO method for the $^3\Pi$-states are shown in Fig. 13. The optimized nuclear parameters Z_a and Z_b from the MO-LCDO method are reproduced in Fig. 14.

The potential curves for the two triplet states $1^3\Pi_g$ and $1^3\Pi_u$ calculated by the MO-LCDO method are shown in Fig. 9 together with the coresponding MO-DO results. Because the MO-DO method represents a special case of the MO-LCDO method the energetic results of the last method must be at least as good as the MO-DO results. In the present calculation, however, a MO-LCDO basis set as small as possible has been chosen which does not allow the representation of the HTDO $|3d\pi_g^+)$. Therefore one can understand why for small internuclear distances the MO-DO results are slightly better than the MO-LCDO values for the state $1^3\Pi_g$. The results calculated by the MO-LCDO method for $1^3\Pi_u$ are slightly better for all R than those of Zemke, Lykos and Wahl [37] and nearly equal to those of J. C. Browne [30]; similarly for $1^3\Pi_g$ [33]. However, better results have been obtained by Wright and Davidson [38] with more extensive calculations.

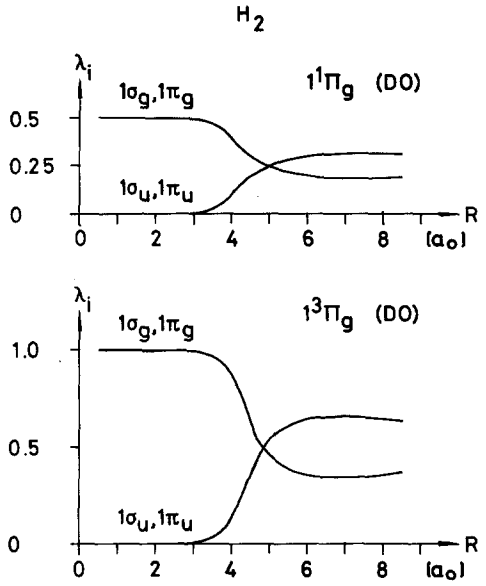

Fig. 11b

Fig. 11a

Fig. 11a and b. Occupation numbers λ_i as functions of the internuclear distance R from the MO-DO calculations for H_2. a) Results for the state $1^3\Pi_g$; b) results for the state $1^1\Pi_g$

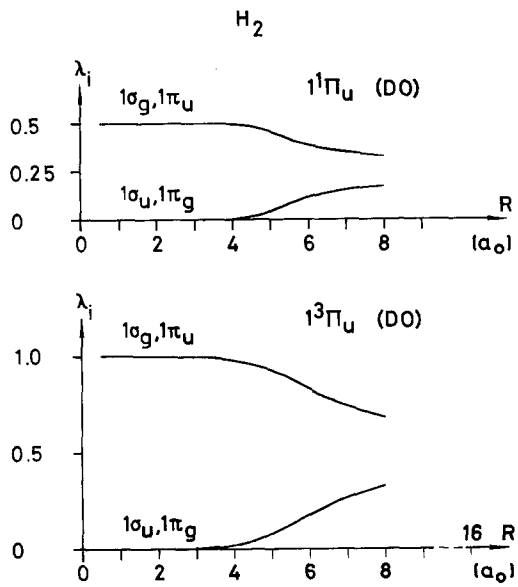

Fig. 12b

Fig. 12a

Fig. 12a and b. Occupation numbers λ_i as functions of the internuclear distance R from the MO-DO calculations for H_2. a) Results for the state $1^3\Pi_u$; b) results for the state $1^1\Pi_u$

4. Discussion

The two-centre basis functions used here are not as variationally flexible as those used e.g. by Rothenberg and Davidson [3] or Kołos and Wolniewicz [21]. However, they have the advantage of being orthogonal functions if they contain the same nuclear charge or, generally, if they are of different symmetry types. They are the exact eigen-

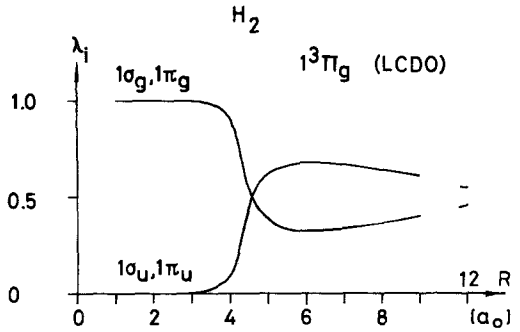

Fig. 13b

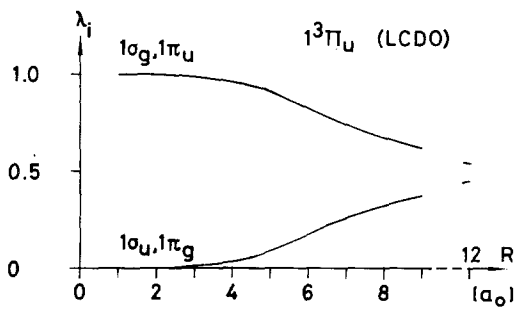

Fig. 13a

Fig. 13a and b. Occupation numbers λ_i as functions of the internuclear distance R from the MO-LCDO calculations for H_2. a) Results for the state $1^3\Pi_u$; b) results results for the state $1^3\Pi_g$

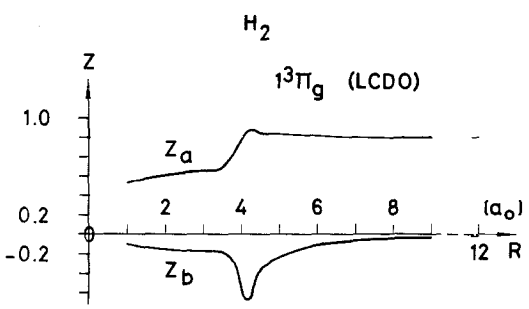

Fig. 14b

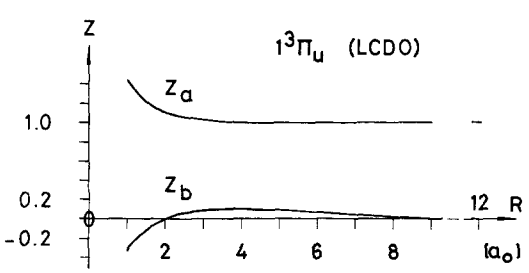

Fig. 14a

Fig. 14a and b. Nuclear charges Z_a and Z_b of the DO's, which have been combined to form the π-functions used in the MO-LCDO calculations for H_2, as functions of the internuclear distance. a) Results for the state $1^3\Pi_u$; b) results for the state $1^3\Pi_g$

functions of a two-centre Hamiltonian operator, so that correlation is the only essential perturbing part of the real H_2 Hamiltonian operator. With the help of optimized DO's the natural orbitals can be interpreted according to, for example, the demi-H_2^+-model and visualized by the well-known H_2^+-type orbitals directly.

4.1. $2^1\Sigma_g^+, 3^1\Sigma_g^+$

The double minimum in the potential curve of the first excited $^1\Sigma_g^+$-state has been interpreted as belonging to the states $1s\sigma_g 2s\sigma_g\ ^1\Sigma_g^+ E$ and $(2p\sigma_u)^2\ ^1\Sigma_g^+ F$ [2, 19–21, 39, 40]. However, no stable state of the united atom He corresponds to the configuration $(2p\sigma_u)^2$. For $R \to \infty$ the separated ions $H^+ + H^-(1s)^2$ belong to this state. Energetically the ionic state lies between the separated atoms H(1s) + H(4s) and H(1s) + H(5s). One would therefore expect a crossing of the potential curves belonging to $^1\Sigma_g^+ F$ and all curves of states which dissociate into H(1s) + H(ns) ($n = 2, 3, 4$), which, however, is avoided because of the non-crossing rule. It will be shown here how this rule influences the potential curves and the corresponding natural orbitals as functions of the internuclear distance.

The calculations result in an optimized nuclear charge parameter Z_{opt} which has indeed the value 0.5 (below $R \approx 2.75$) as in the demi-H_2^+-model. For larger R it increases to a value of about 1.1 and for very large R it changes into the value 1.0 of the free atomic functions. For the state $2^1\Sigma_g^+$ the occupation number curves change quite drastically in the region ($R \approx 3.8$) where the potential curve has a hump. At small R only the first two NO's of gerade symmetry are occupied while the ungerade NO does not participate essentially before this hump (Figs. 1, 2a, b). The most important members of the natural expansion of the wave function expressed by the HTDO's in the region of the minimum of the potential curve of the Rydberg state at $R \approx 2.0$ are:

$$\Psi = 2^{-1/2}\,(|1s\sigma_g\overline{2s\sigma_g}| - |\overline{1s\sigma_g}2s\sigma_g|) \tag{5}$$

In the neighbourhood of the second minimum where the natural expansion is determined mainly by the functions $|1s\sigma_g)$ and $|2p\sigma_u)$ (with a small admixture of other functions with $(2p\sigma_u)^2$ dominating), it has changed to:

$$\Psi = 2^{-1/2}(|1s\sigma_g\overline{1s\sigma_g}| + |2p\sigma_u\overline{2p\sigma_u}|) \tag{6}$$

For $R \to \infty$ this tends to the ionic function

$$\Psi = 2^{-1/2}(|1s_a\overline{1s_a}| + |1s_b\overline{1s_b}|) \tag{7}$$

For even larger R (above $R \approx 10.0$) the NO's $|1\sigma_g)$ and $|2\sigma_g)$ are dominating again in the natural expansion. For the corresponding crossing of the ionic and the homopolar potential curve Lewis [41] gives a value of $R \approx 11.0$. In the limit $R \to \infty$ the wave function is mainly characterized by a valence bond function

$$\Psi \to 1/2\,\{(|1s_a\overline{2b}| - |\overline{1s_a}2b|) + (|1s_b\overline{2a}| - |\overline{1s_b}2a|)\} \tag{8}$$

with

$$|2a) = 2^{-1/2}(|2s_a) - |2p_{0a})) \tag{9}$$

$$|2b) = 2^{-1/2}(|2s_b) - |2p_{0b})) \tag{10}$$

The "crossing" mentioned above is necessary because a lower energy belongs to the function of Eq. (8) than to the ionic function.

The potential curve of the state $3^1\Sigma_g^+$ also possesses a double minimum, which occurs at the smaller internuclear distance of $R \approx 3.4$ in comparison with the state $2^1\Sigma_g^+$. The curves of the occupation numbers of the states $2^1\Sigma_g^+$ and $3^1\Sigma_g^+$ are in accordance with each other up to a shift for $3^1\Sigma_g^+$ to smaller internuclear distances. For both potential curves the first minimum is associated with the NO's $|1\sigma_g)$ and $|2\sigma_g)$ and the region of the second minimum with the NO $|1\sigma_u)$.

The natural expansion for the state $3^1\Sigma_g^+$ changes between $R = 0$ and $R = 2.0$. At $R = 0.5$ the natural expansion in terms of the HTDO basis is given by

$$\Psi = 2^{-1/2}(|1s\sigma_g\overline{3s\sigma_g}| - |\overline{1s\sigma_g}3s\sigma_g|) \tag{11}$$

For $R \approx 1.0$ (and at the equilibrium distance $R \approx 2.0$) an approximate expansion of the wave function is

$$\Psi = 2^{-1/2}(|1s\sigma_g\overline{3d\sigma_g}| - |\overline{1s\sigma_g}3d\sigma_g|) \tag{12}$$

The state $1s3s\,^1S$ of the helium atom, which is of a lower energy than $1s3d\,^1S$, corresponds to the molecular state $1s\sigma_g 3s\sigma_g\,^1\Sigma_g^+$ for small R and changes to $1s\sigma_g 3d\sigma_g\,^1\Sigma_g^+$ at the equilibrium distance. For greater R the contribution of $|2s\sigma_g)$ and $|3s\sigma_g)$ increases and the functions are strongly mixed. From $R \approx 11.0$ the function $|3d\sigma_g)$ takes the place of $|3s\sigma_g)$.

A description of the natural expansion by only a few configurations is not possible for the state $3^1\Sigma_g^+$ because of the mixing of the basis functions. A second maximum of the occupation numbers belonging to $|1\sigma_u)$ and $|2\sigma_u)$ is found at $R \approx 11.0$. This corresponds to a flat minimum in the potential curve at about the same internuclear distance. The wave function there is given approximately by

$$\Psi = 1/2\{(|1s\sigma_g\overline{2s\sigma_g}| - |\overline{1s\sigma_g}2s\sigma_g|) - (|2p\sigma_u\overline{3p\sigma_u}| - |\overline{2p\sigma_u}3p\sigma_u|)\} \tag{13}$$

This function tends to the following valence bond function for $R \to \infty$

$$\Psi \to 1/2\{(|1s_a\overline{2b}| - |\overline{1s_a}2b|) + (|1s_b\overline{2a}| - |\overline{1s_b}2a|)\} \tag{14}$$

where $|2a)$ and $|2b)$ are given by Eqs. (9) and (10). But this is just the behaviour for the limit $R \to \infty$ of the wave function for $2^1\Sigma_g^+$, so that obviously at still greater values of R an avoided crossing of the potential curves of the states $2^1\Sigma_g^+$ and $3^1\Sigma_g^+$ occurs. Davidson [39] has pointed out the possibility of more than two minima for the state $3^1\Sigma_g^+$, but he has only calculated the potential curve up to an internuclear distance $R = 4.5$ [2].

For a description of the state $3^1\Sigma_g^+$ at very large R the function $|2s\sigma_g)$ has to be replaced by $|3d\sigma_g)$ and $|3p\sigma_u)$ by $|4f\sigma_u)$ in Eq. (13). The following equation is valid then:

$$\Psi = 1/2\{(|1s\sigma_g\overline{3d\sigma_g}| - |\overline{1s\sigma_g}3d\sigma_g|) - (|2p\sigma_u\overline{4f\sigma_u}| - |\overline{2p\sigma_u}4f\sigma_u|)\} \tag{15}$$

This expression tends to the following valence bond function for $R \to \infty$:

$$\Psi \to 1/2\ \{(|1s_a\widetilde{\overline{2b}}| - |1s_a\widetilde{2b}|) + (|1s_b\widetilde{\overline{2a}}| - |\overline{1s_b}\widetilde{2a}|)\} \tag{16}$$

with

$$|\widetilde{2a}) = 2^{-1/2}(|2s_a) + |2p_{0a})) \tag{17}$$

$$|\widetilde{2b}) = 2^{-1/2}(|2s_b) + |2p_{0b})) \tag{18}$$

Ionic parts are dominating nowhere in this case. For the slight second maximum in the potential curve at $R \approx 7.0$ an interpretation analogous to that of Wright and Davidson [38] for the case of $1^3\Pi_g$ (see below for the state $2^3\Sigma_g^+$) would be possible if it could be confirmed by a more extended calculation.

4.2. $1^3\Sigma_g^+$, $2^3\Sigma_g^+$

A NO analysis for the states $1^3\Sigma_g^+$ and $2^3\Sigma_g^+$ is contained in the literature only for $R = 2.0$ [3]. The occupation numbers are twofold degenerate here because a wave function belonging to $M_S = 1$ has been chosen (Fig. 4a, b). For small R the first two NO's of gerade symmetry are occupied almost exclusively. The participation of the ungerade NO's does not begin before $R \approx 3.5$ where the changes for $1^3\Sigma_g^+$ with increasing R are quite strong whereas for $2^3\Sigma_g^+$ in the region of the maximum the occupation numbers change less drastically.

The natural expansion for the state $1^3\Sigma_g^+$ expressed in terms of the model functions is given for small R in good approximation by

$$\Psi = |1s\sigma_g 2s\sigma_g| \tag{19}$$

The optimized nuclear parameter Z_{opt} is 0.67 so that Eq. (19) represents a Rydberg state approximately according to the demi-H_2^+-model. For greater R this function changes into

$$\Psi = 2^{-1/2}(|1s\sigma_g 2s\sigma_g| - |2p\sigma_u 3p\sigma_u|) \tag{20}$$

which tends to the following valence bond function for $R \to \infty$:

$$\Psi \to 2^{-1/2}(|1s_a 2b| + |1s_b 2a|) \tag{21}$$

The NO's $|1\sigma_g)$ and $|2\sigma_g)$ for the state $2^3\Sigma_g^+$ mainly consist of the HTDO's $|1s\sigma_g)$ and $|3s\sigma_g)$ at small R. At $R = 2.0$ $|2\sigma_g)$ comprises the function $|3s\sigma_g)$ with an admixture of $|3d\sigma_g)$ and by $R = 2.5$ $|3d\sigma_g)$ predominates. Obviously an avoided crossing of the potential curves belonging to the configurations $(1s\sigma_g 3s\sigma_g)$ and $(1s\sigma_g 3d\sigma_g)$ according to the non-crossing rule has occurred. A complete CI calculation with the restricted basis $|1s\sigma_g)$, $|2s\sigma_g)$, $|3s\sigma_g)$ and $|3d\sigma_g)$ for the states $2^3\Sigma_g^+$ and $3^3\Sigma_g^+$ confirms this behaviour qualitatively [12].

For $R \to \infty$, the determinant $|1s\sigma_g 3s\sigma_g|$ belongs asymptotically to configurations with functions with main quantum numbers 1 and 3:

$$\Psi \to 1/2(|1s_a 3a| + |1s_a 3b| + |1s_b 3a| + |1s_b 3b|) \tag{22}$$

with

$$|3a) = 2^{-1/2}(|3s_a)/\sqrt{3} - |3p_{0a})/\sqrt{2} + |3d_{0a})/\sqrt{6}) \tag{23}$$

$$|3b) = 2^{-1/2}(|3s_b)/\sqrt{3} - |3p_{0b})/\sqrt{2} + |3d_{0b})/\sqrt{6}) \tag{24}$$

On the other hand $|1s\sigma_g 3d\sigma_g|$ goes to pseudo-ionic and valence bond functions consisting of atomic functions with the main quantum numbers 1 and 2. The NO analysis shows that the maximum in the potential curve of the state $2^3\Sigma_g^+$ can be interpreted in such a way that the participation of $|1s\sigma_g 3d\sigma_g|$ does not lead to the correct dissociation into an H atom in the ground state and one in an excited state with the main quantum number $n = 2$; to achieve that, an admixture of $|2p\sigma_u 3p\sigma_u|$ and $|2p\sigma_u 4f\sigma_u|$ is necessary. On the contrary in the state $1^3\Sigma_g^+$ there is *no* essential contribution of parts of the wave function with the wrong dissociative behaviour for any internuclear distance. These results are in accordance with the discussion of Mulliken [5b, 42] on maxima of potential curves which originate from the avoided crossing of two potential curves one of which is attracting and the other repulsive in the first approximation.

4.3. $1^1\Sigma_u^+$, $2^1\Sigma_u^+$

In comparison with the Rydberg states treated up to now the two states $1s\sigma_g 2p\sigma_u\, 1^1\Sigma_u^+ B$ and $1s\sigma_g 3p\sigma_u 2^1\Sigma_u^+ B'$ have unusually large (experimental) equilibrium distances of $R_e = 2.44$ and $R_e = 2.12$ respectively. The deviation from the normal value of about $R_e = 2.0$ is studied with the help of the natural orbital analysis for several internuclear distances.

On account of the qualitative considerations in analogy to those of Wright and Davidson [38] one would expect a maximum in the potential curve of the state $2^1\Sigma_u^+ B'$ as it is calculated here. The occupation numbers and NO's are also in accordance with this expectation. Up to $R = 5.0$ the configuration $(1s\sigma_g 3p\sigma_u)$ predominates in the natural expansion whereas $(2p\sigma_u 2s\sigma_g)$ and $(2p\sigma_u 3d\sigma_g)$ do not contribute significantly before this internuclear distance.

The curves of the two greatest occupation numbers show the special feature that they remain nearly constant in the whole region from $R = 0.5$ to $R = 10.0$ at a value of about 0.5 and 0.0 respectively (Fig. 6). At $R = 11.0$ the two curves approach each other at a value of 0.25. Such constant occupation numbers over such a great region of R occur in the present work only for one other state $1^3\Sigma_u^+$ (see Sect. 4.4). For the state $2^1\Sigma_u^+$ a region of this type only extends to $R \approx 3.0$. At the maximum at $R \approx 5.0$ the two first occupation numbers tend to a common value of 0.25, just like for the state $1^1\Sigma_u^+$ at greater R. According to the non-crossing rule the two curves avoid each other and separate again at greater values of R.

The occupation numbers are fourfold degenerate here; apart from the spin degeneracy, one NSO with a σ_g and one with a σ_u space part belongs to each occupation number. The natural expansion for the state $1^1\Sigma_u^+$ at small R is given in good approximation by

$$\Psi = 2^{-1/2}(|1s\sigma_g \overline{2p\sigma_u}| - |\overline{1s\sigma_g} 2p\sigma_u|) \tag{25}$$

which means that the wave function essentially is in accordance with the model. At $R = 1.75$ the natural expansions change quite drastically while the optimized non-

linear parameter Z_{opt} changes from the Rydberg model parameter $Z_{opt} = 0.5$ to $Z_{opt} = 1.0$. The wave function can then be represented approximately by

$$\Psi = 1/2\{(|1s\sigma_g\overline{2p\sigma_u}| - |\overline{1s\sigma_g}2p\sigma_u|) - (|1s\sigma_g\overline{3p\sigma_u}| - |\overline{1s\sigma_g}3p\sigma_u|)\} \tag{26}$$

The first part of Eq. (26) goes over into an ionic function:

$$(|1s\sigma_g\overline{2p\sigma_u}| - |\overline{1s\sigma_g}2p\sigma_u|) \rightarrow (|1s_a\overline{1s_a}| - |1s_b\overline{1s_b}|) \tag{27}$$

The second part of the wave function in Eq. (26) becomes a mixture of valence bond and ionic functions:

$$|1s\sigma_g\overline{3p\sigma_u}| \rightarrow |1s_a\overline{2a}| - |1s_a\overline{2b}| + |1s_b\overline{2a}| - |1s_b\overline{2b}| \tag{28}$$

The corresponding part of the wave function of Eq. (26) therefore describes the dissociation into H(1s) + H(2s, 2p) correctly. The first ionic part $(1s\sigma_g 2p\sigma_u)$ obviously leads to the relatively broad minimum at an enlarged distance quite analogously to the conditions at the second minimum of the state $2^1\Sigma_g^+$ *E, F*. For medium distances the NO's change quite strongly; the ionic part however can be found constantly in the natural expansion. For the largest nuclear distance considered here ($R = 14.0$) the natural expansion is given by

$$\Psi = 1/2\{(|1s\sigma_g\overline{3p\sigma_u}| - |\overline{1s\sigma_g}3p\sigma_u|) - (|2s\sigma_g\overline{2p\sigma_u}| - |\overline{2s\sigma_g}2p\sigma_u|)\} \tag{29}$$

In the limit $R \rightarrow \infty$ this function goes over into the pseudo-ionic function

$$\Psi \rightarrow 1/2\{(|1s_a\overline{2a}| - |\overline{1s_a}2a|) - (|1s_b\overline{2b}| - |\overline{1s_b}2b|)\} \tag{30}$$

Because the molecule does not dissociate into the ions of high energy the wave function will change once again at a still greater internuclear distance. In addition to the configurations mentioned by Lewis [41] also pseudo-ionic configurations are of importance for the composition of the wave function.

Up to $R = 1.5$ the natural expansion for the state $2^1\Sigma_u^+$ also has a natural expansion of Rydberg character:

$$\Psi = 2^{-1/2}(|1s\sigma_g\overline{3p\sigma_u}| - |\overline{1s\sigma_g}3p\sigma_u|) \tag{31}$$

However in the region of the minimum (up to $R = 3.5$) an ionic part and also a Rydberg part $(1s\sigma_g 4p\sigma_u)$ are added to this:

$$\begin{aligned}\Psi = 2^{-1/2}\{&1/2[(|1s\sigma_g\overline{2p\sigma_u}| - |\overline{1s\sigma_g}2p\sigma_u|) + (|1s\sigma_g\overline{3p\sigma_u}| - |\overline{1s\sigma_g}3p\sigma_u|)] \\ &- (|1s\sigma_g\overline{4p\sigma_u}| - |\overline{1s\sigma_g}4p\sigma_u|)\}\end{aligned} \tag{32}$$

The configuration $(1s\sigma_g 4p\sigma_u)$ also characterizes the increase of the potential curve above the dissociation limit. At the point of the avoided crossing at $R \approx 7.0$ the wave function has just the form of Eq. (29), which describes $1^1\Sigma_u^+$ approximately for great *R*. The state $1^1\Sigma_u^+$ is determined in the same region by the configurations $(1s\sigma_g 2p\sigma_u)$ and $(2p\sigma_u 3d\sigma_g)$ both of which go to valence bond and (pseudo-) ionic configurations respectively with main quantum numbers 1 and 2 belonging to H^-. For very large *R* one has approximately for the state $2^1\Sigma_u^+$

$$\Psi = 1/2\{(|1s\sigma_g\overline{4f\sigma_u}| - |\overline{1s\sigma_g}4f\sigma_u|) - (|2p\sigma_u\overline{3d\sigma_g}| - |\overline{2p\sigma_u}3d\sigma_g|)\} \tag{33}$$

In analogy to Eq. (30) one obtains for $R \to \infty$:

$$\Psi \to 1/2\{(|1s_a\widetilde{2a}| - |\overline{1s}_a\widetilde{2a}|) - (|1s_b\widetilde{2b}| - |\overline{1s}_b\widetilde{2b}|)\} \tag{34}$$

However in addition to this a valence bond part consisting of atomic functions which are participating in Eq. (34) is admixed to the pseudo-ionic part. Also in this case the dissociation is not described correctly by Eq. (34) so that for even larger R the character of the wave function will change once again.

4.4. $1^3\Sigma_u^+$, $2^3\Sigma_u^+$, $3^3\Sigma_u^+$

It is well known that the state $1^3\Sigma_u^+$ possesses a repulsive potential curve. Therefore this state will be compared with the corresponding $1^1\Sigma_u^+$-state and the next two higher $^3\Sigma_u^+$-states which all have potential minima.

It is striking that for the repulsive state $1^3\Sigma_u^+$ the first occupation number is nearly equal to 1.0 for all nuclear distances (see Fig. 8) while all others nearly vanish. This confirms the result of Eliason and Hirschfelder [4]. For $1^1\Sigma_u^+$ a similar behaviour occurs up to a nuclear distance of $R \approx 11.0$, although the shape of the potential curve is quite different in this case. The difference can be seen from the NO's and from the natural expansion (see below).

The natural expansion for $1^3\Sigma_u^+$ is given for all distances in good approximation by

$$\Psi = |1s\sigma_g 2p\sigma_u| \tag{35}$$

which goes over for $R \to 0$ into

$$\Psi \to |1s2p_0| \tag{36}$$

and for $R \to \infty$ into

$$\Psi \to |1s_a 1s_b| \tag{37}$$

The main quantum number of the excited orbital changes from 2 at $R = 0$ and for other finite internuclear distances to 1 of the H-atom orbital at $R \to \infty$.

For the state $2^3\Sigma_u^+$ one has instead of Eq. (35)

$$\Psi = |1s\sigma_g 3p\sigma_u| \tag{38}$$

for $R \to 0$ this function tends to

$$\Psi \to |1s3p_0| \tag{39}$$

For very small values of R the nuclear charge has the optimized value $Z_{\text{opt}} = 0.5$ of the Rydberg model. At the equilibrium distance its value is already 0.78 corresponding to a transition to the separated atoms. The natural expansion of the wave function for large R

$$\Psi = 2^{-1/2}(|1s\sigma_g 3p\sigma_u| - |2p\sigma_u\, 2s\sigma_g|) \tag{40}$$

tends to the following valence bond function in the limit $R \to \infty$:

$$\Psi \to 2^{-1/2}(|1s_a 2b| - |1s_b 2a|) \tag{41}$$

The natural expansion of the wave function of the state $3^3\Sigma_u^+$ is also similar to that given in Eq. (35) for $1^3\Sigma_u^+$:

$$\Psi = |1s\sigma_g 4p\sigma_u| \tag{42}$$

which for $R \to 0$ goes over into

$$\Psi \to |1s4p_0| \tag{43}$$

An exchange of the composition between the greater and lesser occupied NO occurs at the extremal points of the occupation number curves at $R = 5.0$, which coincides with the decrease of the potential curve after the maximum. Concerning the asymptotic behaviour of the natural expansion of the wave function one may expect from its composition at $R = 14.0$ that it will be given by the following equation in analogy to Eq. (40):

$$\Psi = 2^{-1/2}(|1s\sigma_g 4f\sigma_u| - |2p\sigma_u 3d\sigma_g|) \tag{44}$$

Instead of Eq. (41) one has now

$$\Psi \to 2^{-1/2}(|1s_a \widetilde{2b}| - |1s_b \widetilde{2a}|) \tag{45}$$

4.5. $1^3\Pi_u$, $1^3\Pi_g$; $1^1\Pi_u$, $1^1\Pi_g$

In each of the curves of the occupation numbers (see Figs. 11a, b; 12a, b) for all four Π-states one can distinguish two regions: up to $R \approx 3.5$ only one occupation number is essentially different from zero. Therefore the natural expansion is approximated by one determinant e.g. for $1^3\Pi_u$ by

$$\Psi = |1s\sigma_g 2p\pi_u^+| \tag{46}$$

and for the other states by one determinant with $|1s\sigma_g)$ and the DO of the corresponding symmetry for which Z_{opt} has the optimal value 0.5 to 0.6. These are just the conditions of the demi-H_2^+-model. Starting from $R \approx 3.5$ the second occupation number is rapidly increasing. For large R the first two occupation numbers have nearly equal values. Z_{opt} then tends to the nuclear charge 1.0 of the separated atoms. All determinants which may be constructed from the given basis set and which belong to the given symmetry type contribute to the natural expansion with coefficients of equal magnitude:

$$1^3\Pi_u: \quad \Psi = 2^{-1/2}(|1s\sigma_g 2p\pi_u^+| - |2p\sigma_u 3d\pi_g^+|) \tag{47}$$

$$1^1\Pi_u: \quad \Psi = 1/2\{(|1s\sigma_g \overline{2p\pi_u^+}| - |\overline{1s\sigma_g} 2p\pi_u^+|) - (|2p\sigma_u \overline{3d\pi_g^+}| - |\overline{2p\sigma_u} 3d\pi_g^+|)\} \tag{48}$$

$$1^3\Pi_g: \quad \Psi = 2^{-1/2}(|1s\sigma_g 3d\pi_g^+| - |2p\sigma_u 2p\pi_u^+|) \tag{49}$$

$$1^1\Pi_g: \quad \Psi = 1/2\{(|1s\sigma_g \overline{3d\pi_g^+}| - |\overline{1s\sigma_g} 3d\pi_g^+|) - (|2p\sigma_u \overline{2p\pi_u^+}| - |\overline{2p\sigma_u} 2p\pi_u^+|)\} \tag{50}$$

For $R \to \infty$ these functions go over into the following valence bond functions:

$$1^3\Pi_u: \quad \Psi \to 2^{-1/2}(|1s_a 2p\pi_b^+| + |1s_b 2p\pi_a^+|) \tag{51}$$

$$1^1\Pi_u: \quad \Psi \to 1/2\{(|1s_a\overline{2p\pi_b^+}| - |\overline{1s_a}2p\pi_b^+|) + (|1s_b\overline{2p\pi_a^+}| - |\overline{1s_b}2p\pi_a^+|)\} \tag{52}$$

$$1^3\Pi_g: \quad \Psi \to 2^{-1/2}(|1s_a 2p\pi_b^+| - |1s_b 2p\pi_a^+|) \tag{53}$$

$$1^1\Pi_g: \quad \Psi \to 1/2\{(|1s_a\overline{2p\pi_b^+}| - |\overline{1s_a}2p\pi_b^+|) - (|1s_b\overline{2p\pi_a^+}| - |\overline{1s_b}2p\pi_a^+|)\} \tag{54}$$

The curves of the occupation numbers of the Π_u-states and the Π_g-states respectively are quite similar. While for the Π_u-states no crossing points occur, the corresponding curves of the Π_g-states do cross at $R \approx 5.0$. The decreasing of the potential curves after their large maximum coincides with the crossing of the occupation number curves for the Π_g-states. It can be expected that the configuration $(1s\sigma_g 3d\pi_g^+)$ is energetically higher than $(2p\sigma_u 2p\pi_u^+)$ at $R \approx 5.0$ and that one potential curve with a maximum arises from the two [38, 39]. According to this no maximum occurs for the Π_u-states because at $R \approx 5.0$ the configuration $(1s\sigma_g 2p\pi_u^+)$ is present. The slight maximum in the potential curve of the state $1^1\Pi_u$ must have another explanation. The curves of the occupation numbers are nearly equal to those received by the MO-LCDO method (Fig. 13a, b and Figs. 11a and 12a respectively).

The curves of the optimized nuclear charges as functions of the distance R (Fig. 14a: $1^3\Pi_u$; Fig. 14b: $1^3\Pi_g$) show the transition to LCAO functions corresponding to the strong change of the curves of the occupation numbers. For each of the DO's of π-type one of the two nuclear charges becomes equal to 1.0 while the other approximates 0 for $R \to \infty$. For very small R the nuclear charge Z_a takes on values greater than 1.0 while Z_b compensates for this value with a negative charge so that the whole nuclear charge is nearly one at each centre for $1^3\Pi_u$. At the equilibrium distance, Z_a and Z_b have LCAO-values while the corresponding parameters for $1^3\Pi_g$ have the values of 0.6 and -0.1 which are quite similar to the demi-H_2^+-model charges. In the region of the maximum of the potential curve the nuclear charges rapidly change from these to the LCAO-values.

For the elucidation of the difference between the DO's and the LCAO's the overlap integral between the two functions $|2p\pi_u)_{\mathrm{DO}}$ and $|\pi_u 2p)_{\mathrm{LCAO}}$ as well as between $|3d\pi_g)_{\mathrm{DO}}$ and $|\pi_g 2p)_{\mathrm{LCAO}}$ has been maximized for several R. For this reason Z_{DO} has been kept constant and Z_{LCAO} has been optimized. Each of the LCAO's has been represented by two atomic $2p$-functions. For the π_g-function the optimized parameter is approximately equal to 1.0 for the whole region of R and also the overlap integral approximates 1.0. The DO and the LCAO show a great similarity in this case. On the contrary for the π_u-functions the optimal parameter differs from 1.0, and the overlap integral is much smaller, than in the case of the π_g-functions. This behaviour is in accordance with the better representation of the $1^3\Pi_g$-state in comparison with the $1^3\Pi_u$-state by the DO's while $1^3\Pi_u$ is well described only by the more flexible LCDO's.

5. Conclusion

The special features like humps and double minima of most of the potential curves of the excited states examined can be correlated with striking alterations in the curves of the two greatest occupation numbers. However in general an additional consideration of the main parts of the natural expansion and their limiting behaviour is necessary for the understanding of these properties.

All but the Σ_u^+-states can be described by the demi-H_2^+-model for small internuclear distances including the equilibrium value $R_e = 2.0$. For the state $1^1\Sigma_u^+$ the wave function is of a mainly ionic type in the region of the minimum. The common optimal nuclear charge for the $^1\Sigma_u^+$-states is given by that of the separated atoms, which is approached also in the calculations of the $^3\Sigma_u^+$-states, For the higher Rydberg states the configurations of other states with the same symmetry have to be considered.

Avoided crossings of the potential curves of the $^1\Sigma_g^+$- and $^3\Sigma_g^+$-states respectively can be seen from the natural expansion. In the case of the state $3^1\Sigma_g^+$ these lead to a third flat minimum. For greater internuclear distances configuration mixing occurs in general; the natural expansion is mainly determined by two configurations for the lower states only. So in the region of the second minimum of the state $2^1\Sigma_g^+$ an ionic part is admixed to the natural expansion, like for the $1^1\Sigma_u^+$ state near its broad minimum. The decrease of the potential curves with a hump can be attributed to such a part of the natural expansion which allows for a correct dissociation of the states.

From the calculations of the $^3\Pi$-states it seems that for an improvement of the potential curves for medium internuclear distances one has to replace the DO's by LCDO's which allow a flexible transition to LCAO functions.

Acknowledgement. The financial support by the Deutsche Forschungsgemeinschaft and the Sonderforschungsbereich Theoretische Chemie for computer time on CD 3300 of the University of Mainz, CD 6600 of Regionales Rechenzentrum Stuttgart and TR 440 of Deutsches Rechenzentrum Darmstadt as well as the assistance in these computing centres is gratefully acknowledged by the authors.

References

1. Davidson, E. R.: Advan. Quantum Chem. **6**, 235 (1972)
2. Davidson, E. R.: J. Chem. Phys. **35**, 1189 (1961)
3. Rothenberg, S., Davidson, E. R.: J. Chem. Phys. **45**, 2560 (1966)
4. Eliason, M. A., Hirschfelder, J. O.: J. Chem. Phys. **30**, 1397 (1959)
5. Mulliken, R. S.: a) J. Am. Chem. Soc. **86**, 3183 (1964); b) J. Am. Chem. Soc. **88**, 1849 (1966); c) J. Am. Chem. Soc. **91**, 4615 (1969)
6. Hylleraas, E. A.: Z. Physik **71**, 739 (1931)
7. Lassettre, E. N., Peek, J. M.: J. Chem. Phys. **38**, 2395 (1963)
8. Teller, E., Sahlin, H. L.: Physical Chemistry, Vol. 5, p. 35, Eyring, H., Ed. New York: Academic Press 1970
9. Helfrich, K., Hartmann, H.: Theoret. Chim. Acta (Berl.) **16**, 263 (1970)
10. Kehl, S., Helfrich, K., Hartmann, H.: Theoret. Chim. Acta (Berl.) **21**, 44 (1971)
11. Helfrich, K.: Theoret. Chim. Acta (Berl.) **21**, 381 (1971)

12. Kehl, S.: Energieberechnung und Darstellung der natürlichen Spinorbitale mit Zweizentrenfunktionen für angeregte Zustände des Wasserstoffmoleküls, Dissertation Frankfurt am Main 1974
13. Helfrich, K.: Entwicklung natürlicher Spinorbitale kleiner zweiatomiger Moleküle nach verallgemeinerten Zweizentrenfunktionen, Habilitationsschrift Frankfurt am Main 1971
14. Helfrich, K.: Theoret. Chim. Acta (Berl.) **30**, 169 (1973)
15. Bingel, W. A., Kutzelnigg, W.: Advan. Quantum Chem. **5**, 201 (1970)
16. Kutzelnigg, W.: Theoret. Chim. Acta (Berl.) **1**, 327 (1963)
17. Wigner, E., von Neumann, J.: Z. Physik **30**, 467 (1929)
18. Bingel, W. A.: Theoret. Chim. Acta (Berl.) **16**, 319 (1970)
19. Gerhauser, J., Taylor, H. S.: J. Chem. Phys. **42**, 3621 (1965)
20. Boye, R. J.: J. Mol. Spectry. **26**, 36 (1968)
21. Kołos, W., Wolniewicz, L.: J. Chem. Phys. **50**, 3228 (1969)
22. a) Herzberg, G.: Molecular spectra and molecular structure I. Spectra of diatomic molecules, 2nd Ed. Princeton, New Jersey: van Nostrand 1950
b) Sharp, T. E.: Atomic Data **2**, 119 (1971)
23. Huestis, D. L., Goddard, III, A.: Chem. Phys. Letters **16**, 157 (1972)
24. Wakefield, C. B., Davidson, E. R.: J. Chem. Phys. **43**, 834 (1965)
25. Kołos, W., Wolniewicz, L.: J. Chem. Phys. **48**, 3672 (1968)
26. Namioka, T.: J. Chem. Phys. **43**, 1636 (1965)
27. Monfils, A.: Bull. Acad. Roy. Soc. Belg. **54** (1), 44 (1968)
28. Taylor, H. S.: J. Chem. Phys. **39**, 3375 (1963)
29. Shull, H.: J. Am. Chem. Soc. **82**, 1287 (1960)
30. Hirschfelder, J. O., Linnett, J. W.: J. Chem. Phys. **18**, 130 (1950)
31. Browne, J. C.: J. Chem. Phys. **41**, 1583 (1963)
32. Browne, J. C.: Phys. Rev. **138A**, 9 (1965)
33. Kołos, W., Wolniewicz, L.: J. Chem. Phys. **45**, 509 (1966)
34. Kołos, W., Wolniewicz, L.: J. Chem. Phys. **43**, 2429 (1965)
35. Browne, J. C.: J. Chem. Phys. **40**, 43 (1964)
36. Rothenberg, S., Davidson, E. R.: J. Chem. Phys. **44**, 730 (1966)
37. Zemke, W. T., Lykos, P. G., Wahl, A. C.: J. Chem. Phys. **51**, 5635 (1969)
38. Wright, W. M., Davidson, E. R.: J. Chem. Phys. **43**, 840 (1965)
39. Davidson, E. R.: J. Chem. Phys. **33**, 1577 (1960)
40. Kołos, W.: Intern. J. Quantum Chem. **2**, 471 (1968)
41. Lewis, J. T.: Proc. Phys. Soc. **A68**, 632 (1955)
42. Mulliken, R. S.: Phys. Rev. **136A**, 962 (1964)

Received March 29, 1976/September 2, 1976